We are grateful to two anonymous referees for their constructive suggestions and thoughtful comments.

The author response (AC) to the individual referee comments (R) is provided below.

Response to Referee #1

Major comments:

R1: Section 4.1 is not clear enough. The authors state that NAO and NIÑO3.4 indexes are correlated with TOC, but no evidences are presented in the article. Only visual correlations are mentioned. What about statistical correlation? Furthermore, Figs. 3 and 4 are difficult to read. Please, clarify the y-axes for ELOs and EHOs.

AC: Following the referees suggestion we provide additional statistics and their discussion in the revised version of the manuscript (Sect. 4.1). In both winter and spring the NAO Index correlates negatively with the frequency of EHOs and positively with the frequency of ELOs, indicating an increase (decrease) in the frequency of high ozone events during a negative (positive) NAO phase and vice versa for low ozone events, manifested also in the seasonal means (see Table 1 in the revised manuscript). Further differences in the occurrence and detection frequency of NAO fingerprints are captured in the correlation analysis, with overall stronger correlations during winter than spring. This is further explored in Figure 7 (added to the revised manuscript), which shows the fraction of EHOs and ELOs during wintertime positive and negative NAO events: more (less) EHOs during NAO- (NAO+) phases and vice versa for ELOs. We note that correlation analysis between ENSO and column ozone (or the frequency of EHOs and ELOs) is less conclusive than that for the NAO, which is attributed to the rather small number of strong ENSO events.

The captions of Figures 3 and 4 (and corresponding supplemental figures) have been updated according to the referees comment to better explain the y-axes, e.g. for Figure 3 the new caption reads: 'Fingerprints' of the NAO and ENSO as detected for Boulder in the seasonal frequency time series of EHOs (right axis, top to bottom) and ELOs (left axis, bottom to top) for (A) winter (DJF), and (B) spring (MAM). Bottom panels (C) and (D) show 'fingerprints' in seasonal mean column ozone. Filled circles denote visible 'fingerprints' and crosses denote not visible 'fingerprints'. NAO positive (negative) phase is indicated for winter in red (blue) and for spring in orange (light blue), ENSO positive phase is indicated for winter (spring) in green (light green).

R1: A deeper discussion should be performed in section 4.3. The authors attribute to the large spatial distance the absence of fingerprints during NAO and ENSO events at the five sites. I partially agree with the explanation of regional effects. As Figure 6 is, practically, limited to certain months, I think more analysis should be performed for particular events. Is there any difference (meteorological, synoptic,...) between those events discernible at the five sites and those only visible in northern sites or the eastern sites,...?? In this sense, are these differences in line with the results shown of Table 3? Some sites present good relationships in winter or spring for the extreme influence, are these similarities translated to the fingerprints during certain events?

AC: Correlations of daily TOC among sites are rather noisy (local effects, temporal lags due to dynamics), vertical investigations are limited by the absence of vertically resolved ozone profiles, and seasonal comparisons between years with 'fingerprints' and without are restricted to a small sample size (i.e., few missing fingerprints on a site basis). Nevertheless a comparison of CDFs on site basis between neighboring years with 'fingerprints' and without reveals the absence of high or low ozone events associated with the NAO or ENSO (see Figure S6, which will has been included in the supplemental material of the revised manuscript). Thus instead of individual effects, we quantify the overall contribution of extremes to seasonal mean column ozone by calculating the influence of ELOs and EHOs at each site.

R1: I miss more comments about the interesting topic of double tropopauses (e.g., Randel et al., 2007;Pan et al., 2009). Previous studies have shown that intrusions of subtropical air above the extratropical tropopause produce a decrease in the ozone levels (e.g., Castanheira et al. 2012), and being more frequent with NAO positive phases (e.g., Mateos et al., 2014). It is not necessary a complete analysis of these events (maybe, it is beyond the aims of the article), but these events should be more clearly mentioned in the discussion since they are clearly latitudinal dependent and can play a notable role in the differences among the five sites.

AC: We agree with the referee that the subject of double tropopauses (DTROP) and their influence on column ozone received increasing attention in recent years. While a detailed event based analysis is beyond the scope of the present work, we agree that a section detailing the relationship between DTROP events and TOC and their relation to the 5 US sites strengthens the manuscript. The following paragraphs have been added to Sect. 4.3 of the revised manuscript.

'Several studies have linked the occurrence of multiple tropopauses to Rossby wave breaking events along the subtropical jet (Homeyer and Bowman, 2013, and references therein), and to associated tropospheric intrusions (e.g., Pan et al., 2009); climatological maxima in multiple tropopause occurrence have been linked to observed changes in vertical profiles of satellite-observed trace gases that are consistent with air from the tropical tropopause layer being drawn into the region between the two tropopauses; specifically, climatological ozone mixing ratios in midlatitude multiple tropopause regions are substantially lower than those in regions with a single tropopause (Schwartz et al., submitted). Schwartz et al estimated that in NH winter midlatitudes, when multiple tropopauses are most common, climatological ozone values can be as much 20% lower that they would be without multiple tropopauses.

These results are consistent with the observed association of lower column ozone with multiple tropopauses (e.g., Castanheira et al., 2012;Mateos et al., 2014). Mateos et al. (2014) also noted more common occurrence of such tropospheric intrusion events during NAO positive phases, suggesting a role for dynamical modes such as NAO and ENSO in modulating multiple tropopause occurrence and thus their corresponding effects on ozone.

In addition, there is a maximum in multiple tropopause occurrence frequency over the US in winter and spring, extending poleward from the region where upper tropospheric jets are most common (Manney et al., 2014). Boulder, Nashville, and Wallops Island are near the latitude of maximum multiple tropopause occurrence just poleward of the subtropical upper tropospheric jet, while Bismarck and Caribou are at the northern edge of the region of enhanced multiple

tropopause activity (Manney et al., 2014), and are thus less frequently affected by processes in multiple tropopause regions.'

Minor comments:
R1: Abstract. "from the five US sites...". I understand that no more sites have ozone records since 1960 in the US. Is this true?

AC: Correct. The five sites analyzed in this study are the only ones that provide continuous total ozone observations back to the 1960s within the continental US.

R1: Figure 1. Although the coordinates of each site are indicated in the figure, I'd appreciate if the map is geo-localized.

AC: Figure 1 has been updated according to the referee's suggestion.

R1: Figure 2. Please, add some discussion about this figure. For instance, the authors can discuss the latitudinal or longitudinal dependence of the threshold values among the five sites, and others.

AC: Additional discussion of Figure 2 is provided in the revised manuscript, see paragraph below.

'Thresholds for ELOs and EHOs, as well as long-term monthly mean values for the five US sites, are shown Figure 2. Here the well-known seasonal cycle with ozone minima in fall and maxima in spring, as well as the latitudinal dependence of total ozone mean values and thresholds (i.e., higher TOC at northern sites (Bismarck and Caribou) due to transport of ozone rich air from high latitudes) is visible.'

R1: Tables 1 and 2. More statistical information should be given in these Tables. Although the standard error is given for each trend, I'd appreciate the knowledge of, e.g., the p value. Maybe it is possible to reduce these two tables to only one. With one table is easier to compare the two periods analyzed.

AC: Tables 1 and 2 have been merged and p-values have been added (new Table 2).

Response to Referee #2

General comments
R2: 1. Abstract p. 21067, line 9-12: I object the statement: The Loess smoothed trend components show a decline of total ozone between the 1970s and 2000s and a "stabilization" at lower levels in recent years which is confirmed by linear trend analysis (see below).

AC: This statement has been removed in the revised manuscript.

R2: 2. p. 21073, line 12: “Our main interest in this study lies in the trend component of the STL-decomposition”: I see the values using STL plots to illustrate the relations between ozone time series and fingerprints (such as in the figures 5 and S5) but the scientific interpretation of “trend component” of total ozone time series analysis is obscure to me (see below) as the procedure leads to smoothing over the effects of many different processes (see below)

AC: We agree with the referee that the STL-trend components are not reliable measures for TOC trends as they are rather TOC residual trends that are smoothed after the seasonal cycle is removed, which removes individual short-term variability associated with various meteorological effects. Throughout the paper STL-trend components are mainly used to provide a secondary assessment for ‘fingerprints’ of NAO and ENSO events corroborating the EVT analysis. Statistical trend calculations in the presented manuscript (time periods for which will be updated according to the referees’ comment, see below) are solely based on linear regression models. For clarity we will remove any ‘trend interpretation’ of the STL-trends and use STL-trend components solely for demonstration of the ‘fingerprint’ detection.

R2: 3. p. 21075, line 13 “Fingerprints” of NAO and ENSO in the frequency distribution of extreme events: “The NAO fingerprints are in broad agreement with those for European sites and satellite data, and p. 21076, line 6 are in good agreement with findings for European sites and satellite data”: please provide more specific statements

AC: This section has been updated according to the referees’ comment, see paragraph below:

‘The NAO ‘fingerprints’ identified in the US column ozone records are in broad agreement with those for European sites and satellite data. Appenzeller et al. (2000) were among the first to report on the influence of the NAO on column ozone over Europe, based on their analysis of the world’s longest total ozone record, Arosa, Switzerland. Rieder et al. (2010a) extended these investigations toward low and high ozone values and Rieder et al. (2011) documented the influence of the NAO in its positive (reduced column ozone, reduced frequency of high ozone events) and negative (increased column ozone, increased frequency of high ozone events) phases for five European ground based sites in 1970-2010. These authors report a similar number of detected ‘fingerprints’ and occasional misses at individual sites due to local effects. Frossard et al. (2013) extended investigations to larger spatial scales by analyzing the NIWA assimilated total ozone data set in 1979-2007. These authors report that the ‘fingerprint’ of the NAO is of similar spatial extent for both mean values and ozone extremes, but that the magnitude of influence on total ozone is larger for extremes than mean values. These results are in broad agreement with those presented here for the US long-term ozone records, documenting the significant influence of the NAO on column ozone variability throughout northern mid-latitudes.’

R2: 4. p. 21077, line 12ff: I cannot follow the arguments: “show that the strong decrease during 1980s and 1990s came to a halt around the turn of the century”: I see the Fig 5 for Boulder is a decreasing tendency until 1996 followed by sort of a “jump” and a new “decreasing tendency” staring again around 1997 which is similar for Wallops Island (Fig S5) whereas Bismark might show a tendency for an upward trend after 1993, less pronounced in Nashville. Because of the subjectivity of such statements I recommend to avoid STL plots for statements regarding “trend

analyses" whereas the plots can be used to illustrate the relation between fingerprints and ozone time series. Additionally I find it difficult to interpret the "trend component" from STL plots as the procedure basically "smoothes" over different processes, e.g. the Pinatubo effect.

AC: See earlier comment regarding STL-trend components.

R2: 5. p. 21078, line 18 ff: I cannot see the rational of the selection of the periods of linear trends analyses, namely 1970-2000 and 1990-2010: I don't believe that maximum ODS was "around 2000": What means "maximum ODS": emissions or EESC? To my knowledge EESC for mid-latitude was peaking around the middle of the last decade (1997 ?). The start of the second period in 1990 includes the low ozone values generally attributed to the volcanic eruption of Pinatubo and therefore these low values are expected to contribute to the upward trends. If a statement in connection with anthropogenic ozone destruction is attempted I recommend to use linear trend analysis for 1970-1995 and 1995-2010 leading to a more positive trend.

AC: We agree with the referees remarks regarding the time periods chosen for trend analysis. According to the referees suggestion we updated the calculations for the periods 1970-1995 and 1996-2010 in accordance with the EESC maximum for middle latitudes found in ~1996-97. While the magnitude of the trends is affected by this change the overall conclusions of the trend analysis are not. For 1970-1995, the period with almost linearly increasing ODS and significant mid-latitude ozone losses in the early 1980s and 1990s (following the El Chichon and Mt. Pinatubo eruptions), ozone trends vary between -2.8 and -4.8 percent per decade among the sites and seasons. All sites, except Caribou, show larger negative trends in spring compared to winter. For the more recent past, 1996-2010, we find positive trends at most sites, an anticipated result since stratospheric chemistry in this period is impacted by slowly but steadily declining ODS. Positive trends at the majority of sites indicate that ozone has stopped declining over the US, particularly during winter, suggesting that chemical depletion may have ceased. Nevertheless, since the trend estimates over the period 1996-2010 during spring typically do not exceed the standard errors and show insignificant p-values, there is no clear evidence that significant ozone recovery has been identified yet.

In addition to the new trend analysis we keep the original trend analysis for the periods 1970-2000 and 1990-2010 for the supplemental material of the manuscript to emphasize that although trends are mostly of the same sign they differ in magnitude and significance among seasons and time periods analyzed.

R2: 6. P. 21079, line 17.: I suggest to mention here again that the record low values in total ozone in northern mid-latitudes are commonly attributed to the effect of Pinatubo aerosols.

AC: The Mt. Pinatubo reference has been included in Sect. 4.3 of the revised manuscript.

R2: 7. P. 21082, line 5-8: please explain how the changes in frequencies of ELOs and EHOs are connected with the expansion of tropical belt and the contraction of the northern polar band.

AC: This section has been extended in the revised manuscript see paragraph below.

‘Further, ELOs are indicative of the extension of the subtropical jet to the north of the station, which brings in tropical air masses with low ozone content, while EHOs are indicative of an equatorward excursion of the polar jet and advection of O_3-rich air masses from high latitudes. The changing frequency of ELOs and EHOs is thus in agreement with the notion of the expansion of the tropical band and contraction of the northern polar band (e.g., Hudson et al., 2006;Seidel et al., 2008). During the 1980-2000 period, when ozone depletion was strongest, individual years still show a net positive contribution of the extremes to seasonal mean column ozone, demonstrating the importance of individual negative NAO and warm ENSO events for ozone variability.’

The influence of the North Atlantic Oscillation and El Niño-Southern Oscillation on mean and extreme values of column ozone over the United States

I. Petropavlovskikh[1], R. Evans[2], G. McConville[1], G.L. Manney[3,4], H.E. Rieder[5,6]

[1] {Cooperative Institute for Research in Environmental Sciences, University of Colorado, Boulder, CO 80309, USA}
[2] {NOAA Earth System Research Laboratory, Boulder, CO 80305, USA}
[3] {NorthWest Research Associates, Socorro, NM 87801, USA}
[4] {Department of Physics, New Mexico Institute of Mining and Technology, Socorro, NM 87801, USA}
[5] {Wegener Center for Climate and Global Change and IGAM/Institute of Physics, University of Graz, 8010 Graz, Austria}
[6] {Lamont-Doherty Earth Observatory of Columbia University, Palisades, NY 10964, USA}

Correspondence to: I. Petropavlovskikh (irina.petro@noaa.gov)

Abstract

Continuous measurements of total ozone (by Dobson spectrophotometers) across the contiguous United States (US) began in the early 1960s. Here, we analyze temporal and spatial variability and trends in total ozone from the five US sites with long-term records. While similar long-term ozone changes are detected at all five sites, we find differences in the patterns of ozone variability on shorter time scales. In addition to standard evaluation techniques, STL-decomposition methods (Seasonal Trend decomposition of time series based on LOcally wEighted Scatterplot Smoothing (LOESS)) are used to address temporal variability and ~~trends in the~~'fingerprints' of dynamical features in the Dobson data. ~~The LOESS-smoothed trend components show a decline of total ozone between the 1970s and 2000s and a 'stabilization' at lower levels in recent years, which is also confirmed by linear trend analysis.~~ Methods from statistical extreme value theory (EVT) are used to characterize days with high and low total ozone (termed EHOs and ELOs, respectively) at each station and to analyze temporal changes in the frequency of ozone extremes and their relationship to dynamical features such as the North Atlantic Oscillation and El Niño Southern Oscillation. A comparison of the 'fingerprints' detected in the frequency distribution of the extremes with those for standard metrics (i.e., the mean) shows that more 'fingerprints' are found for the extremes, particularly for the positive phase of the NAO, at all five US monitoring sites. Results from the STL-decomposition support the findings of the EVT analysis. Finally, we analyze the relative influence of low and high ozone events on seasonal mean column ozone at each station. The results show that the influence of ELOs and EHOs on seasonal mean column ozone can be as much as ±5 percent, ~~or~~ about ~~twice~~ as large as the overall long-term decadal ozone trends.

1. Introduction

Long-term monitoring of ozone is critical because it is instrumental in controlling the levels of ultraviolet radiation reaching the planet's surface and thus plays an important role in the existence of life on Earth (e.g., Tourpali et al., 2009;Bais et al., 2011;McKenzie et al., 2011). The 25th anniversary of the Montreal protocol (signed in 1987) marked an important milestone in the phasing out of man-made chemicals such as chlorofluorocarbons (CFCs), commonly referred to as ozone depleting substances (ODS). ODS have very long life times in the stratosphere (some as long as 100 years); they are lofted throughout the stratosphere from the tropical troposphere, transported into the middle and high latitudes, and recirculate, providing chlorine (and bromine) atoms for chemical ozone destruction (WMO, 2011;Rigby et al., 2013).

Analyses of inter-annual and long-term variability in total column ozone on regional (e.g., Mäder et al., 2007;Rieder et al., 2010b, a;Rieder et al., 2011;Fitzka et al., 2014) and global (e.g., Frossard et al., 2013;Rieder et al., 2013) scales have been presented in a number of recent studies. There is now a broad consensus that long-term negative ozone trends are dominated by ODS, while short-term trends and variability, particularly at mid-latitudes, are also significantly influenced by synoptic-scale meteorological variability (e.g., Steinbrecht et al., 1998;Shepherd, 2008), decadal climate variability (e.g., Chandra et al., 1996;Hood, 1997) and dynamical modes such as the El Niño-Southern Oscillation (ENSO) (e.g., Brönnimann et al., 2004;Ziemke et al., 2010;Hood et al., 2010;Gabriel et al., 2011), the North Atlantic Oscillation (NAO)/Arctic Oscillation (AO) (e.g., Appenzeller et al., 2000;Thompson and Wallace, 2000) and volcanic eruptions (e.g., Jaeger and Wege, 1990;Solomon, 1999;Robock, 2000;Mäder et al., 2007). For the European Sector it has been reported that dynamical variability accounts for about a third of the observed ozone changes between the 1970s and 1990s (e.g., Mäder et al., 2007;Wohltmann et al., 2007). The particular importance of dynamical changes for column ozone at mid-latitudes has also been highlighted in more recent

work that attributes the slight increase in column ozone since the 1990s primarily to dynamics and to a lesser extent to the decrease in ODS (after their peak around 1997) (e.g., Harris et al., 2008;Hegglin and Shepherd, 2009;WMO, 2007, 2011).

In addition, recent work analyzing the tails of the ozone distribution (i.e., the extremes) in relation to the bulk properties (i.e., the mean) showed that analysis of the tails allows for a more systematic attribution of ozone changes to dynamical features than mean value analysis can achieve (e.g., Rieder et al., 2010b, a;Rieder et al., 2011;Frossard et al., 2013;Rieder et al., 2013). These studies also showed that even moderate NAO and ENSO events can have significant effects on the mid-latitude ozone field.

Furthermore, it has been noted that while column ozone at northern mid-latitudes reached its lowest values in the early 1990s, following the 1991 eruption of Mount Pinatubo, the effect of this eruption was partially masked by atmospheric dynamics in the southern hemisphere (e.g., Schnadt Poberaj et al., 2011;Rieder et al., 2013), again emphasizing the importance of atmospheric dynamics to ozone trends and variability.

In this paper we attempt to assess the information contained in the integrated total ozone column derived from the continental US network of Dobson measurements. We discuss interannual variability in column ozone, how it has changed over the last 50 years, what controls it, and how trends are statistically related to dynamical and chemical proxies.

2. Data

2.1 Ground-based total ozone data sets

Continuous measurements of total column ozone (TOC) over the continental United States began in the early 1960s. Individual measurements were also made earlier at some sites, but more sporadically and mainly in conjunction with the International Geophysical Year 1957.

The backbone of the World Meteorological Organizations (WMO) ozone monitoring network is the Dobson Ozone Spectrophotometer, an instrument developed in the 1920s specifically for high accuracy measurements of total column ozone (e.g., Dobson, 1957, 1968). The concept of the Dobson measurement is the differential absorption of ozone at selected wavelengths in the solar ultraviolet spectrum. Two pairs, where one spectral range absorbs light more strongly than the other, are combined to minimize the effect of aerosol interference on the measurements. Measurements made using the direct solar beam are used to determine the TOC based on Lambert-Beers law, while measurements made with the scattered light from the zenith are converted to a TOC value based on the statistics of quasi-simultaneous measurements of both direct sun and zenith.

Operational instrument calibration is maintained by monthly tests with reference and discharge lamps, plus regular inter-comparison with two standard instruments: D083 (World Primary Standard) or D065 (World Secondary Standard). The calibration of the Primary Standard is maintained by Langley Plot Campaigns at the National Oceanic and Atmospheric Administration's Earth System Research Laboratory Mauna Loa Observatory (Hawaii).

In the contiguous US, column ozone has been measured routinely at five observational sites (Bismarck, ND; Boulder, CO; Caribou, ME; Wallops Island, VA; Nashville, TN) since the 1960s. In this study we analyze the total ozone records from these five sites spanning from the 1960s through 2012. A detailed overview on geographical location and information on record length, data completeness and time series properties of the individual station records is provided in Figure 1.

2.2 Proxies for atmospheric dynamics

There is now a broad consensus that long-term trends in total ozone are driven primarily by changes in the atmospheric concentration of ozone depleting substances (ODS) (WMO,

2011). Nevertheless, active research in the field showed that besides ODS, several other processes have significant influence on total ozone changes and variability. The 11-year solar cycle, the Quasi-Biennial Oscillation (QBO) and volcanic eruptions are among the most prominent explanatory variables often used to describe the influence of atmospheric variability on column ozone (WMO, 2011). At mid-latitudes other dynamical features also show significant influence on column ozone on seasonal and inter-annual time scales. In particular, synoptic scale meteorological variability, described by, e.g., the North Atlantic Oscillation (NAO) (e.g., Appenzeller et al., 2000;Orsolini and Doblas-Reyes, 2003;Rieder et al., 2010a;Frossard et al., 2013;Rieder et al., 2011), and climate modes such as the El Niño-Southern Oscillation (ENSO) (e.g., Rieder et al., 2013;Rieder et al., 2010a;Brönnimann et al., 2004) have been shown to significantly influence ozone variability and trends.

In the present study we focus particularly on the influence of atmospheric dynamics on variability and trends in column ozone over the US. To this aim we use a set of indices describing ENSO and NAO modes on seasonal basis in the statistical analysis. For ENSO we are using the seasonal NINO3.4 Index provided by NOAA's Climate Prediction Center – available at http://www.cpc.ncep.noaa.gov/data/indices/3mth.nino34.81-10.ascii.txt. For the NAO we are using the seasonal station-based index (based on the difference of normalized sea level pressures between Ponta Delgada, Azores and Stykkisholmur/Reykjavik, Iceland) provided by the NCAR/UCAR climate data center – available at https://climatedataguide.ucar.edu/sites/default/files/climate_index_files/nao_station_seasonal_1.txt).

3. Methods

3.1 Extreme Value Statistics

Recent work has introduced concepts of statistical extreme value theory (EVT) into the field of total ozone research (Rieder et al., 2010b, a;Rieder et al., 2011;Frossard et al.,

2013;Rieder et al., 2013;Fitzka et al., 2014). Here we build on these methodologies to analyze extreme low and high ozone events (termed ELOs and EHOs, respectively), in the US long-term total ozone records.

The generalized Pareto distribution (GPD) is a commonly used distribution in the framework of extreme value theory (e.g., Davison and Smith, 1990;Ribatet et al., 2009) because it arises as the natural distribution for the exceedance of a random variable (here total ozone) over a threshold. Below we briefly describe the modeling procedure for values over a threshold. Note that the modeling for values below a threshold is precisely the same, the only thing to be done is to negate the values and apply exactly the same procedure as for values above a high threshold as min (xi)=-max(xi).

The GPD, which is the limiting distribution of exceedances over a threshold, is defined as:

$$F(x) = 1 - \left[1 + \xi \frac{x-u}{\sigma}\right]^{-\frac{1}{\xi}}, \sigma > 0,\ x > u, 1 + \xi \frac{x-u}{\sigma} > 0\ , \qquad \text{(Eq. 1)}$$

where x are daily data (here total ozone), u is the threshold value and σ and ξ are the scale (a measure of the spread of the distribution of x) and shape (which is determining the shape of the distribution rather than shifting it as u does or shrinking/stretching it as σ does) parameters, respectively.

Threshold values u are determined on a monthly basis and interpolated to daily values following the procedure described by Rieder et al. (2010b). ~~For convenient reference,~~ ~~t~~Thresholds for ELOs and EHOs, as well as long-term monthly mean values for the five US sites, are shown Figure 2. Here the well-known seasonal cycle with ozone minima in fall and maxima in spring, as well as the latitudinal dependence of total ozone mean values and thresholds (i.e., higher TOC at northern sites (Bismarck and Caribou) due to transport of ozone rich air from high latitudes) is visible.

Following Rieder et al. (2010b) total ozone observations at the individual US sites are categorized in three groups (see Eqs. 2-4),

$$ELO = \{x(t): x(t) < u_{LOW}(t)\}, \quad \text{(Eq. 2)}$$

$$EHO = \{x(t): x(t) > u_{HIGH}(t)\}, \quad \text{(Eq. 3)}$$

$$NEO = \{x(t): u_{LOW}(t) \leq x(t) \leq u_{HIGH}(t)\}, \quad \text{(Eq. 4)}$$

where, $x(t)$ is the column ozone amount at a given day, $u_{LOW}(t)$ and $u_{HIGH}(t)$ are the thresholds for low and high ozone on a given day, and ELO, EHO, NEO denote days with low, high, and non-extreme ozone, respectively. The frequency of low and high ozone events is discussed below in the context of dynamical features (see Sect. 4.1).

3.2 Seasonal Trend decomposition of Time series based on LOESS (STL)

Seasonal Trend decomposition of time series based on LOESS (LOcally wEighted Scatterplot Smoothing) (e.g., Cleveland et al., 1990) decomposes a data record (here ozone) into seasonality, trend and residual components. When applied to the US column ozone data it returns a well-known picture: (i) a strong seasonal cycle with maxima in spring and minima in winter/fall, in accordance with the understanding of the influence of the Brewer-Dobson circulation on column ozone (transport of ozone-rich air towards northern-mid-latitudes during boreal winter); (ii) a negative trend-component dominated by the influence of ODS on column ozone, and (iii) a highly variable residual component representing the effects of local scale meteorology on column ozone. An example of an STL-decomposition for the site in Boulder, CO is shown in Figure S1 in the supplemental material of this article. For a more detailed description of the STL-procedure we refer the interested reader to the paper of Cleveland et al. (1990) describing the method.

STL-trend components represent smoothed TOC residuals after the seasonal cycle is removed, and are thus not reliable measures for TOC trend analysis. Statistical trend analysis

in this manuscript is solely based on linear regression analysis (see Section 4.4). Here we utilize STL because the resulting trend component provides a more detailed picture of the seasonal and interannual variability in the overall TOC time series compared to, e.g., a simple linear trend component, and thus is suitable for the secondary assessment of 'fingerprints' of NAO and ENSO events as long-term time series variability is preserved.

4. Results

The main goal of this paper is to analyze the influence of dynamical features such as NAO and ENSO on column ozone over the US. To this aim EVT modeling and STL decomposition are applied to the long-term total ozone time series to derive 'fingerprints' of the dynamical covariates.

4.1 'Fingerprints' of NAO and ENSO in the frequency distribution of extreme events

In Section 3.1 we described the classification of total ozone observations into days with extreme low, extreme high and non-extreme ozone. Here we focus on the frequency distribution of the extremes and analyze the influence of ENSO and NAO events on column ozone at the five US ozone monitoring sites. As the general features are very similar among the individual sites, we show mainly the results for Boulder and Caribou, which give the envelope of column ozone observations over the US, in the main body of the paper. For convenient reference, illustrations for other sites are available in the supplemental material for this article. In Figs. 3 and 4 we plot the observed frequency of ELOs, NEOs and EHOs as time series for Boulder and Caribou (the results for the remaining sites are shown in Figs. S2-S4). Next, we turn to 'fingerprints' of atmospheric dynamics in the frequency distribution of EHOs and ELOs at these sites.

First, we turn to the North Atlantic Oscillation which is the leading mode in the Atlantic sector, influencing the direction and intensity of the tropospheric jet stream (e.g., Orsolini and Limpasuvan, 2001) and representing the main driver of the inter-annual variability in storm tracks during the cold season (e.g., Lau, 1988). A positive NAO phase leads to lower ozone over Europe and the US and higher ozone over Labrador and Greenland, and vice versa for a negative NAO phase (see Rieder et al., 2010b and references therein; and Frossard et al., 2013 for a spatial representation of NAO influence on column ozone at northern mid-latitudes).

The North Atlantic Oscillation in its negative phase (NAO index < -1, marked with blue (winter) and light blue (spring) dots in Figs. 3 and 4) leads to higher column ozone over the United States during winter and spring. Conversely, a 'fingerprint' of the NAO in its positive phase (NAO index > 1, marked with red (winter) and orange (spring) dots in Figs. 3 and 4) is seen as lower ozone over the US in the individual station records. Over the study period (1963-2012), the NAO has been in a strongly positive phase (NAO index > 1) 16 times during winter and 12 times during spring. While all but one of the wintertime events are captured in the frequency of ELOs at multiple sites, 2 out of the 12 spring events remain undetected (1982 and 1994) at any of the five US sites (see Figure 6). The correlation analysis confirms the relationship between column ozone and the NAO phase (see Table 1). In both winter and spring the NAO Index correlates negatively with the frequency of EHOs and positively with the frequency of ELOs, indicating an increase (decrease) in the frequency of high ozone events during a negative (positive) NAO phase and vice versa for low ozone events, manifested also in the seasonal means.

It has been noted that the NAO has tended towards a more positive phase in recent decades (e.g., Hurrel, 1995; Thompson and Wallace, 2000), concomitant with a strengthening of the northern polar vortex. Nevertheless, a strongly negative NAO phase (NAO index < -1) is found 10 times during winter and 5 times during spring (roughly half the rate of positive

phase events) in 1963-2012. Out of the 10 wintertime events 8 are discernible in the frequency distribution of extreme total ozone, with the winters of 1973/74 and 2010/11 being absent. The missing NAO 'fingerprint' in winter 2010/11 is not surprising given the unusual dynamical conditions in the Arctic in this year, which led to a particularly strong stratospheric polar vortex and record Arctic ozone losses (e.g., Manney et al., 2011), counteracting the dynamic enhancement of column ozone due to the NAO. Out of the 5 springtime negative NAO events, 3 can be identified in (most of) the five US monitoring sites, with 2005 and 2006 missing. As was the case in 2011, the particularly cold conditions in the Arctic spring of 2005 likely contribute to the missing NAO 'fingerprint'. Differences in the occurrence and detection frequency of NAO fingerprints are captured in the correlation analysis, with overall stronger correlations during winter than spring. This is further explored in Figure 7, which shows the fraction of EHOs and ELOs during wintertime positive and negative NAO events: more (less) EHOs during NAO- (NAO+) phases and vice versa for ELOs.

The NAO 'fingerprints' identified in the US column ozone records are in broad agreement with those for European sites and satellite data. Appenzeller et al. (2000) were among the first to report on the influence of the NAO on column ozone over Europe, based on their analysis of the world's longest total ozone record, Arosa, Switzerland. Rieder et al. (2010a) extended these investigations toward low and high ozone values and Rieder et al. (2011) documented the influence of the NAO in its positive (reduced column ozone, reduced frequency of high ozone events) and negative (increased column ozone, increased frequency of high ozone events) phases for five European ground based sites in 1970-2010. These authors report a similar number of detected 'fingerprints' and occasional misses at individual sites due to local effects. Frossard et al. (2013) extended investigations to larger spatial scales by analyzing the NIWA assimilated total ozone data set in 1979-2007. These authors report that the 'fingerprint' of the NAO is of similar spatial extent for both mean values and ozone extremes, but that the magnitude of influence on total ozone is larger for extremes than mean

values. These results are in broad agreement with those presented here for the US long-term ozone records, documenting the significant influence of the NAO on column ozone variability throughout northern mid-latitudes.

~~The NAO 'fingerprints' identified in the US column ozone records are in broad agreement with those for European sites and satellite data confirming the significant influence of the NAO on column ozone variability throughout northern mid-latitudes.~~

Next we turn to the El Niño-Southern Oscillation. Warm ENSO events are triggered by a high contrast between tropical and extratropical Pacific sea-surface temperatures, which are known to affect mid-latitudes (in particular the North Pacific) via changes in the Hadley cell and Rossby wave generation (e.g., Trenberth, 1998;Alexander et al., 2002). During warm ENSO events, the meridional circulation in the stratosphere leads to enhanced ozone transport from the tropics to middle and high latitudes and a warmer lower stratosphere, both of which tend to increase mid-latitude ozone (Rieder et al., 2013, and references therein).

The warm ENSO phase (El Niño, NINO3.4 index > 0.7) is, as expected, associated with higher ozone over the US during winter/spring, visible in the frequency distribution of the extremes. During the study period, moderate to strongly positive ENSO events have been recorded 11 times during winter and 4 times during spring. Most wintertime events (except those in 1983, 1992 and 1995) and springtime events (except 1983 and 1992) can be identified in the frequency distribution of ozone extremes. The absence of ENSO 'fingerprints' in the remaining three years is consistent with their occurrence immediately after the two major volcanic eruptions of the last century (El Chichon in 1982 and Mt. Pinatubo in 1991), when the effects of the volcanic eruptions (enhanced ozone depletion on sulfate aerosols) would have masked the dynamical signal. As was the case for the NAO, the ENSO results for the US sites are in good agreement with findings for European sites and satellite data (e.g., Rieder et al., 2010a;Rieder et al., 2013), illustrating the importance of ENSO in modulating column

ozone at northern mid-latitudes. The correlation analysis between ENSO and column ozone (or the frequency of EHOs and ELOs) is less conclusive then for the NAO, probably because of the rather small number of strong ENSO events.

At all sites we find a more consistent presence of 'fingerprints' of NAO and ENSO in extreme values of column ozone (upper panels in Figs. 3 and 4) than in its mean values (lower panels of Figs. 3 and 4). While the extremes show a pronounced response (increasing or decreasing frequency) to the prevailing ENSO and NAO phases, the mean values often do not show large differences compared to neighboring years without ENSO or NAO events. This is particularly evident for NAO+ events, where about twice as many events were detected in the frequency distribution of the extremes than in the seasonal mean values.

4.2 'Fingerprints' of atmospheric dynamics in the STL decomposition

Here we contrast the findings of the EVT-based analysis with results from the STL-decomposition approach. In Figure 5 we show the anomaly of the trend components of the STL-decomposition for the two selected US sites, Boulder and Caribou, as above in the EVT-analysis (the results for the remaining sites are shown in Fig. S5). While the overall trend curves show a steady decline that is most pronounced in the 1980s and 1990s, as expected from the strong negative influence of ODS on column ozone (e.g., WMO, 2011), there is also a large degree of inter-annual variability in these curves. This variability is not related to seasonality in the ozone field, since the seasonal component has been removed from the data prior to the trend computations within the STL-procedure.

As for the EVT-analysis we now identify 'fingerprints' of ENSO and NAO events in the STL trend component. The colored vertical bars in Figs. 5a,c mark positive and negative winter- and spring time NAO events. The analysis of the STL trend-component shows that positive NAO events are associated with a decreasing tendency in the trend curve, and thus with lower column ozone, while negative NAO events are associated with an increasing

tendency in the STL trend component, and thus with higher column ozone. Fig. 5b,d show the corresponding results for warm ENSO events, which tend to enhance column ozone.

The good agreement between the results in Figure 5 with those from the EVT-analysis (Figs. 3 and 4) provides further evidence for the significant influence of strong NAO and ENSO events on column ozone variability over the continental US.

~~The STL trend-decomposition anomalies also show that the strong negative tendencies present during the 1980s and 1990s came to halt around the turn of the century. In recent years the trend components at all sites shows a high degree of interannual variability, though with an overall stabilization at lower column ozone levels.~~

~~This result suggests that although there is as yet no definitive sign of ozone recovery in the US column ozone records, the period of pronounced ozone loss is seen to have come to halt, a feature that has also been seen in other ground based sites and in results from state-of-the-art chemistry climate model calculations (e.g., SPARC-CCMVal, 2010;Eyring et al., 2010). We will evaluate this qualitative finding in more detail in Sect. 4.4.~~

4.3 Similarities and differences among the individual monitoring sites

Despite the overall similarity in trends and patterns of variability, it is important to note that 'fingerprints' of individual NAO and ENSO events are not always found at all 5 stations analyzed. Figure 6 provides a summary of all major ENSO and NAO events over the 1963-2012 time period and their detection (or absence) in the individual station records. Solid squares in Figure 6 mark 'fingerprints' detected while open squares mark 'absent' fingerprints at individual sites. The majority of ENSO and NAO events are detected at all five US total ozone monitoring sites, but some individual events are not discernible at individual (or multiple) sites such as, e.g., the negative NAO event of spring 1996. The absence of individual 'fingerprints' is not too surprising given the large spatial distance between

individual sites and their regional location (see Figure 1). The occasional masking of large scale ozone variability by localized synoptic-scale meteorology (e.g., the influence of the subtropical jets and localized tropopause variations) is associated with the regional patterns of advection and convergence or divergence that are related to changes in tropospheric and stratospheric pressure systems as has been previously reported for other than US regions (e.g., Koch et al., 2005;Mäder et al., 2007;Wohltmann et al., 2007).

Direct correlations of daily TOC between sites are rather inconclusive due to the difficulty in accounting for local meteorological effects at a station or temporal lags between stations due to transport. Unfortunately, vertical investigations are limited by the absence of vertically resolved ozone profiles at most of the stations (except for Boulder, CO). In addition, seasonal comparisons between years with 'fingerprints' and without are restricted to a small sample size (i.e., few missing fingerprints on a site basis). Nevertheless, a comparison of cumulative distribution functions (CDFs) on site basis between neighboring years with and without 'fingerprints' reveals the absence of high or low ozone events associated with the NAO or ENSO (see Figure S6 in the supplemental material). Thus, instead of individual effects, we quantify the overall contribution of extremes to seasonal mean column ozone by calculating the influence of ELOs and EHOs at each site.

~~The absence of individual 'fingerprints' is not too surprising given the large spatial distance among individual sites (see Figure 1) and is attributed to regional effects such as masking by synoptic-scale meteorology (e.g., the influence of the subtropical jets and localized tropopause variations) and regional patterns of advection and convergence or divergence related to changes in tropospheric and stratospheric pressure systems, which exert local influences on column ozone, as has been previously reported for other regions (e.g., Koch et al., 2005;Mäder et al., 2007;Wohltmann et al., 2007).~~ Several studies have linked the occurrence of multiple tropopauses to Rossby wave breaking events along the subtropical jet

(Homeyer and Bowman, 2013, and references therein), and to associated tropospheric intrusions (e.g., Pan et al., 2009); climatological maxima in multiple tropopause occurrence have been linked to observed changes in vertical profiles of satellite-observed trace gases that are consistent with air from the tropical tropopause layer being drawn into the region between the two tropopauses; specifically, climatological ozone mixing ratios in midlatitude multiple tropopause regions are substantially lower than those in regions with a single tropopause (Schwartz et al., submitted). Schwartz et al estimated that in NH winter midlatitudes, when multiple tropopauses are most common, climatological ozone values can be as much 20% lower that they would be without multiple tropopauses.

These results are consistent with the observed association of lower column ozone with multiple tropopauses (e.g., Castanheira et al., 2012;Mateos et al., 2014). Mateos et al. (2014) also noted more common occurrence of such tropospheric intrusion events during NAO positive phases, suggesting a role for dynamical modes such as NAO and ENSO in modulating multiple tropopause occurrence and thus their corresponding effects on ozone.

In addition, there is a maximum in multiple tropopause occurrence frequency over the US in winter and spring, extending poleward from the region where upper tropospheric jets are most common (Manney et al., 2014). Boulder, Nashville, and Wallops Island are near the latitude of maximum multiple tropopause occurrence just poleward of the subtropical upper tropospheric jet, while Bismarck and Caribou are at the northern edge of the region of enhanced multiple tropopause activity (Manney et al., 2014), and are thus less frequently affected by processes in multiple tropopause regions.

The absence of individual 'fingerprints' on site basis and their underlying cause is of general interest, though beyond the spatial and climatological scope of the presented study. Nevertheless further analysis (including ~~also~~ vertical information from sounding profiles) is

suggested for future site specific analysis addressing effects of local dynamics on column ozone variability.

4.4 Influence of extreme events on ozone mean values and trends

In this section we turn the focus to column ozone trends at the five US Dobson sites.

To analyze the influence of extremes (both low and high) on ozone trends we contrast linear trends for the entire observational time series (i.e., all observational data included) with trends for time series with extremes removed. We focus on two main time periods: ~~(1)~~ 1970-~~2000~~1995, ~~the period with almost linearly increasing ODSs and thus largest ozone depletion, and (2) the period from 1990-2010,~~ with almost linearly increasing ODS, which ~~spans~~ includes the peak in ozone depletion (following the Mt. Pinatubo eruption), and a second period, 1996-2010, that extends from the maximum in ODSs (~~2000~~1996/1997) to current conditions. Results for each site during winter and spring are given in Table~~s~~ 2~~ and 3~~.

During the 1970-1995 period, with almost linearly increasing ODS and significant mid-latitude ozone losses in the early 1980s and 1990s (following the El Chichon and Mt. Pinatubo eruptions), ~~(1970-2000, Table 1)~~ ozone trends vary between -2.8 and -~~3.5~~4.8 percent per decade among the sites and seasons (Table 2). All sites except Caribou show larger negative trends in spring than in winter, consistent with results from European mid-latitude sites (e.g., Rieder et al., 2010b, 2011). We argue that this qualitative difference between Caribou and the other US sites is determined by geography. Caribou is the northernmost US monitoring site and thus is more frequently affected by transport of air masses out of the Arctic polar regions in winter and spring than the other stations; such Arctic air may, in particularly cold winters, carry the signature of chemical ozone depletion. The more southerly sites are usually most strongly influenced by mid-latitude ozone-rich air masses (e.g., Manney et al., 2014), though they may also show effects of transport of low-ozone air from low latitudes and accompanying troposphere to stratosphere exchange.

Comparing the entire observational records with those with extremes removed, we find that trends are only about half as strong in the latter case. This is particularly interesting as for the magnitude of EHOs or ELOs no statistically significant trend (at a 95%-level) is found over 1970-~~2000~~1995. The individual time series show the well-known pattern of large interannual variability but no robust increase (or decrease) in the average magnitude of the extremes themselves. Thus the influence of extremes on seasonal mean column ozone (see below) can be understood as a function of their occurrence frequency, driven by chemical ozone depletion and dynamics.

Turning now to the more recent past, i.e., ~~the last two decades~~1996-2010 (Table ~~3~~2), we find positive trends at ~~all~~ most sites, an ~~unsurprising~~ anticipated result since stratospheric chemistry in this period is impacted by slowly but steadily declining ODS. ~~result since the period with largest mid-latitude ozone losses in the early 1990s has been followed by a period of slowly but steadily declining ODS.~~ The key interest in the trends for ~~1990~~1996-2010 is thus not the sign of the trends but their significance. Observational and modelling studies suggest that chemical ozone depletion ceased to increase around the turn of the century (e.g., WMO, 2011), but whether significant ozone recovery has started is still undetermined. Positive trends at the majority of sites indicate that ozone has stopped declining over the US, particularly during winter, suggesting that chemical depletion may have ceased (Table 2). ~~The majority of positive signs in Table 2 3 indicate that ozone has stopped declining over the US, particularly during winter season, suggesting that chemical depletion may have ceased~~. Nevertheless, since the trend estimates over the ~~20~~15-year period ~~1990~~1996-2010 are not significant at the 95% level (see *p*-values in Table 2) ~~typically do not exceed the standard errors (given in parentheses in Table 2),~~ there is no clear evidence that significant ozone recovery has started yet. As was the case for 1970-~~2000~~1995, the trends are much smaller (a factor of 2-3) if extremes are removed from the records. Again we investigate whether significant changes occurred in the extremity of ELOs and EHOs and, as for the 1970-~~2000~~ 1995 period, we find

large interannual variability in the magnitude of lows and highs (driven by dynamics and chemistry) though no significant trends at rigorous test levels (i.e., 95%).

Discriminating the effects of the individual dynamical proxies on column ozone is difficult because: (i) 'fingerprints' for multiple proxies are found in several years (e.g., a strongly positive NAO and a warm ENSO phase) and (ii) the occurrence frequency of the individual 'fingerprints' is highly variable. Also correlations between sites are rather noisy on daily time scales (local effects) and seasonal comparisons between years with 'fingerprints' and 'without' are restricted to a small sample size (i.e., too few missing fingerprints on site basis). Thus ~~Instead~~instead of individual effects, we quantify the overall contribution of extremes to seasonal mean column ozone by calculating the influence of ELOs and EHOs at each site:

$$I_{ELOs} = \left(\frac{M_s - M_{sELO(ex)}}{M_s}\right) * 100 \qquad \text{(Eq. 5)}$$

$$I_{EHOs} = \left(\frac{M_s - M_{sEHO(ex)}}{M_s}\right) * 100 \qquad \text{(Eq. 6)}$$

where I_{ELOs} (I_{EHOs}) is the influence of extreme low (high) total ozone on seasonal mean column ozone (M_s) in percent, and $M_{sELO(ex)}$ ($M_{sEHO(ex)}$) is the seasonally averaged column ozone with ELOs (EHOs) excluded from the time series. In Figures 8 and 9 we show the influence of ELOs and EHOs on winter and spring column ozone, respectively. While EHOs are the dominant influence in the early and late parts of the station records, the time period from 1980-2000 is dominated by the influence of ELOs, consistent with the nearly linear increase in ODSs and their importance to column ozone changes in this time period. During this period of strong ozone depletion, however, individual years still show a net positive effect of the extremes on seasonal mean column ozone, highlighting the importance of dynamical factors, such as warm ENSO events (e.g., spring 1986 and 1998), on column ozone variability. The influence of ELOs and EHOs on seasonal mean ozone is bound by about ±5 percent, thus about as large as the overall long-term trend values given in Table ~~1~~2.

Next we analyze the pattern correlation of the net contribution of the extremes (i.e., I_{ELOs} + I_{EHOs}) among individual sites. The seasonal pattern correlations among individual sites are summarized in Table 3. Pattern correlations are highest for neighboring sites, i.e., Boulder-Bismarck and Nashville-Wallops Island. Caribou is again an exception in this respect, with a seasonally dependent correlation with the other sites. During winter, the correlation at Caribou is highest with the eastern sites (Nashville and Wallops Island), while during spring, the correlation is highest with the western sites (Bismarck and Boulder), suggesting that Caribou is under the influence of the same air masses as the eastern/western sites during different seasons. Examinations of the overall correlations for each decade of the record (not shown here) indicates that the correlation between Boulder and Nashville (particularly in winter) increases with time (i.e., it is higher in the 1990s and 2000s than in the 1970s and 1980s), while the correlation between Nashville and Wallops Island slightly decreased in recent decades (in both winter and spring), consistent with Boulder and Nashville being more frequently influenced by similar air masses in recent years. Recent operational changes at Caribou, resulting in reduced sampling frequency, significantly affect the correlation between Caribou and Wallops Island, thus highlighting the importance of continuous and frequent ozone observations for both trend analysis and assessment of relationships between measurements at different sites.

5. Discussion and Conclusions

In this study we analyze data from the five long-term Dobson stations across the contiguous US to investigate the influence of the Northern Atlantic Oscillation (NAO) and the El Niño-Southern Oscillation (ENSO) on total ozone variability and trends since the 1960s. In addition to standard evaluation techniques we utilize a STL-decomposition method (Seasonal-Trend decomposition procedure based on LOESS) and statistical extreme value theory (EVT)

to address the temporal variability and trends in the Dobson data in relation to synoptic-scale meteorological and climate variability.

The results show that 'fingerprints' of the dynamical features are better captured in the tails (i.e., the extremes) than in the bulk (i.e., the mean) of the observational records, a result in broad agreement with earlier work for European monitoring sites (Rieder et al., 2010a;Rieder et al., 2011) and satellite data (e.g., Frossard et al., 2013;Rieder et al., 2013). 'Fingerprints' of individual ENSO and NAO events are coherently captured at a majority of the sites, indicating the large-scale influence of these features on column ozone. The observed increase in the frequency of ELOs and decrease in the frequency of EHOs from the 1970s on is in agreement with the notion of increasing ODS. Further, ELOs are indicative of the extension of the subtropical jet to the north of the station, which brings in tropical air masses with low ozone content, while EHOs are indicative of an equatorward excursion of the polar jet and advection of O_3-rich air masses from high latitudes. The changing frequency of ELOs and EHOs is thus in agreement with the notion of the expansion of the tropical band and contraction of the northern polar band (e.g., Hudson et al., 2006;Seidel et al., 2008). During the 1980-2000 period, when ozone depletion was strongest, individual years still show a net positive contribution of the extremes to seasonal mean column ozone, demonstrating the importance of individual negative NAO and warm ENSO events for ozone variability.

In agreement with earlier work we find significant negative trends in column ozone over the US in 1970-~~2000~~ 1995 (the period with almost linearly increasing ODS). Although column ozone values over the US ceased to decrease around the turn of the century, the observational records for ~~1990~~1996-2010 generally show positive, but insignificant, trends, and thus do not yet show a clear signature of the onset of ozone recovery. Trends derived excluding extremes from the records are much smaller than those derived from the full records, consistent with previous results for other regions and datasets. The contribution of

low and high ozone events to winter and spring mean column ozone is bound by about ±5 percent, a value ~~about twice as large~~roughly comparable ~~as~~ to the mean negative trends in 1970-~~2000~~1996 (and larger than trends in individual sub-periods), indicating the importance of dynamics to ozone variability and trends.

Pattern correlations of the contribution of low and high ozone events to seasonal mean column ozone are highest for neighboring sites (i.e., Bismarck-Boulder and Nashville-Wallops Island), though not homogenous among sites (e.g., seasonally dependent and time varying among individual sites). Trends for individual sub-periods (i.e., 1970-1995 and 1996-2010 (Table 2); 1970-2000 and 1990-2010 (see supplemental material)) are mostly of the same sign at all sites, but differ in magnitude and significance among seasons and time periods analyzed.

The results presented here highlight the importance of a continued spatially-distributed long-term ozone monitoring program to address future ozone changes and to detect and confirm the onset and progress of ozone recovery in the context of the Montreal Protocol.

Acknowledgements

The authors wish to express appreciation to the NOAA Weather Service personnel whose efforts in making the Dobson ozone measurements over sixty years allow us to study some of the longest atmospheric constituent time series in existence. The authors thank the NOAA Climate Prediction Center and NCAR/UCAR climate data center for providing ENSO and NAO Indices used in this study via their respective data portals. The authors are grateful to two anonymous referees for helpful comments during the discussion phase in ACPD.

References

Alexander, M. J., Tsuda, T., and Vincent, R. A.: Latitudinal variations observed in gravity waves with short vertical wavelengths, Journal of the Atmospheric Sciences, 59, 1394-1404, 2002.

Appenzeller, C., Weiss, A. K., and Staehelin, J.: North Atlantic oscillation modulates total ozone winter trends, Geophysical Research Letters, 27, 1131-1134, 2000.

Bais, A. F., Tourpali, K., Kazantzidis, A., Akiyoshi, H., Bekki, S., Braesicke, P., Chipperfield, M. P., Dameris, M., Eyring, V., Garny, H., Iachetti, D., Jockel, P., Kubin, A., Langematz, U., Mancini, E., Michou, M., Morgenstern, O., Nakamura, T., Newman, P. A., Pitari, G., Plummer, D. A., Rozanov, E., Shepherd, T. G., Shibata, K., Tian, W., and Yamashita, Y.: Projections of UV radiation changes in the 21st century: impact of ozone recovery and cloud effects, Atmospheric Chemistry and Physics, 11, 7533-7545, DOI 10.5194/acp-11-7533-2011, 2011.

Brönnimann, S., Luterbacher, J., Staehelin, J., Svendby, T. M., Hansen, G., and Svenoe, T.: Extreme climate of the global troposphere and stratosphere in 1940-42 related to El Nino, Nature, 431, 971-974, 10.1038/nature02982, 2004.

Castanheira, J. M., Peevey, T. R., Marques, C. A. F., and Olsen, M. A.: Relationships between Brewer-Dobson circulation, double tropopauses, ozone and stratospheric water vapour, Atmospheric Chemistry and Physics, 12, 10195-10208, DOI 10.5194/acp-12-10195-2012, 2012.

Chandra, S., Varotsos, C., and Flynn, L. E.: The mid-latitude total ozone trends in the northern hemisphere, Geophysical Research Letters, 23, 555-558, 1996.

Cleveland, R. B., Cleveland, W. S., McRae J. A., and Terpenning I.: STL: A Seasonal-Trend Decomposition Procedure Based on Loess, Journal of Official Statistics, 6, 3-73, 1990.

Davison, A. C., and Smith, R. L.: Models for exceedances over high thresholds (with Discussion), Journal of the Royal Statistical Society Series B, 52, 393-442, 1990.

566 Dobson, G. M. B.: Observers' handbook for the ozone spectrophotometer, Ann. Int. Geophys.
567 Year, 5, 46-89, 1957.
568 Dobson, G. M. B.: 40 Years Research on Atmospheric Ozone at Oxford - a History, Appl
569 Optics, 7, 387-&, Doi 10.1364/Ao.7.000387, 1968.
570 Eyring, V., Cionni, I., Bodeker, G. E., Charlton-Perez, A. J., Kinnison, D. E., Scinocca, J. F.,
571 Waugh, D. W., Akiyoshi, H., Bekki, S., Chipperfield, M. P., Dameris, M., Dhomse, S., Frith,
572 S. M., Garny, H., Gettelman, A., Kubin, A., Langematz, U., Mancini, E., Marchand, M.,
573 Nakamura, T., Oman, L. D., Pawson, S., Pitari, G., Plummer, D. A., Rozanov, E., Shepherd,
574 T. G., Shibata, K., Tian, W., Braesicke, P., Hardiman, S. C., Lamarque, J. F., Morgenstern,
575 O., Pyle, J. A., Smale, D., and Yamashita, Y.: Multi-model assessment of stratospheric ozone
576 return dates and ozone recovery in CCMVal-2 models, Atmospheric Chemistry and Physics,
577 10, 9451-9472, 10.5194/acp-10-9451-2010, 2010.
578 Fitzka, M., Hadzimustafic, J., and Simic, S.: Total ozone and Umkehr observations at Hoher
579 Sonnblick 1994–2011: Climatology and extreme events, Journal of Geophysical Research,
580 119, 739-752, 10.1002/2013JD021173, 2014.
581 Frossard, L., Rieder, H. E., Ribatet, M., Staehelin, J., Maeder, J. A., Di Rocco, S., Davison, A.
582 C., and Peter, T.: On the relationship between total ozone and atmospheric dynamics and
583 chemistry at mid-latitudes - Part 1: Statistical models and spatial fingerprints of atmospheric
584 dynamics and chemistry, Atmospheric Chemistry and Physics, 13, 147-164, 10.5194/acp-13-
585 147-2013, 2013.
586 Gabriel, A., Kornich, H., Lossow, S., Peters, D. H. W., Urban, J., and Murtagh, D.: Zonal
587 asymmetries in middle atmospheric ozone and water vapour derived from Odin satellite data
588 2001-2010, Atmospheric Chemistry and Physics, 11, 9865-9885, DOI 10.5194/acp-11-9865-
589 2011, 2011.
590 Harris, N. R. P., Kyro, E., Staehelin, J., Brunner, D., Andersen, S. B., Godin-Beekmann, S.,
591 Dhomse, S., Hadjinicolaou, P., Hansen, G., Isaksen, I., Jrrar, A., Karpetchko, A., Kivi, R.,

592 Knudsen, B., Krizan, P., Lastovicka, J., Maeder, J., Orsolini, Y., Pyle, J. A., Rex, M.,
593 Vanicek, K., Weber, M., Wohltmann, I., Zanis, P., and Zerefos, C.: Ozone trends at northern
594 mid- and high latitudes - a European perspective, Annales Geophysicae, 26, 1207-1220, 2008.
595 Hegglin, M. I., and Shepherd, T. G.: Large climate-induced changes in ultraviolet index and
596 stratosphere-to-troposphere ozone flux, Nature Geoscience, 2, 687-691, 10.1038/ngeo604,
597 2009.
598 Homeyer, C. R., and Bowman, K. P.: Rossby Wave Breaking and Transport between the
599 Tropics and Extratropics above the Subtropical Jet, Journal of the Atmospheric Sciences, 70,
600 607-626, Doi 10.1175/Jas-D-12-0198.1, 2013.
601 Hood, L. L.: The solar cycle variation of total ozone: Dynamical forcing in the lower
602 stratosphere, Journal of Geophysical Research-Atmospheres, 102, 1355-1370, 1997.
603 Hood, L. L., Soukharev, B. E., and McCormack, J. P.: Decadal variability of the tropical
604 stratosphere: Secondary influence of the El Nino-Southern Oscillation, Journal of
605 Geophysical Research-Atmospheres, 115, Doi 10.1029/2009jd012291, 2010.
606 Hudson, R. D., Andrade, M. F., Follette, M. B., and Frolov, A. D.: The total ozone field
607 separated into meteorological regimes - Part II: Northern Hemisphere mid-latitude total ozone
608 trends, Atmospheric Chemistry and Physics, 6, 5183-5191, 2006.
609 Jaeger, H., and Wege, K.: Stratospheric ozone depletion at northern mid-latitudes after major
610 volcanic eruptions, Journal of Atmospheric Chemistry, 10, 273-287, 1990.
611 Koch, G., Wernli, H., Schwierz, C., Staehelin, J., and Peter, T.: A composite study on the
612 structure and formation of ozone miniholes and minihighs over central Europe, Geophysical
613 Research Letters, 32, L12810, 10.1029/2004gl022062, 2005.
614 Lau, N. C.: Variability of the observed midlatitude storm tracks in relation to low-frequency
615 changes in the circulation pattern, Journal of the Atmospheric Sciences, 45, 2718-2743, 1988.

Mäder, J. A., Staehelin, J., Brunner, D., Stahel, W. A., Wohltmann, I., and Peter, T.: Statistical modeling of total ozone: Selection of appropriate explanatory variables, Journal of Geophysical Research-Atmospheres, 112, D11108, 10.1029/2006jd007694, 2007.

Manney, G. L., Santee, M. L., Rex, M., Livesey, N. J., Pitts, M. C., Veefkind, P., Nash, E. R., Wohltmann, I., Lehmann, R., Froidevaux, L., Poole, L. R., Schoeberl, M. R., Haffner, D. P., Davies, J., Dorokhov, V., Gernandt, H., Johnson, B., Kivi, R., Kyro, E., Larsen, N., Levelt, P. F., Makshtas, A., McElroy, C. T., Nakajima, H., Parrondo, M. C., Tarasick, D. W., von der Gathen, P., Walker, K. A., and Zinoviev, N. S.: Unprecedented Arctic ozone loss in 2011, Nature, 478, 469-U465, 10.1038/nature10556, 2011.

Manney, G. L., Hegglin, M. I., Daffer, W. H., Schwartz, M. J., and Santee, M. L.: Climatology of Upper Tropospheric-Lower Stratospheric (UTLS) Jets and Tropopauses in MERRA, Journal of Climate, 27, 3248-3271, 10.1175/JCLI-D-13-00243.1, 2014.

Mateos, D., Antón, M., Sáenz, G., Bañón, M., Vilaplana, J. M., and García, J. A.: Dynamical and temporal characterization of the total ozone column over Spain, Climate Dynamics, 1-10, 10.1007/s00382-014-2223-4, 2014.

McKenzie, R. L., Aucamp, P. J., Bais, A. F., Bjorn, L. O., Ilyas, M., and Madronich, S.: Ozone depletion and climate change: impacts on UV radiation, Photoch Photobio Sci, 10, 182-198, Doi 10.1039/C0pp90034f, 2011.

Orsolini, Y. J., and Limpasuvan, V.: The North Atlantic Oscillation and the occurrences of ozone miniholes, Geophysical Research Letters, 28, 4099-4102, 2001.

Orsolini, Y. J., and Doblas-Reyes, F. J.: Ozone signatures of climate patterns over the Euro-Atlantic sector in the spring, Q J Roy Meteor Soc, 129, 3251-3263, 10.1256/qj.02.165, 2003.

Pan, L. L., Randel, W. J., Gille, J. C., Hall, W. D., Nardi, B., Massie, S., Yudin, V., Khosravi, R., Konopka, P., and Tarasick, D.: Tropospheric intrusions associated with the secondary tropopause, Journal of Geophysical Research-Atmospheres, 114, Doi 10.1029/2008jd011374, 2009.

642 Ribatet, M., Ouarda, T., Sauquet, E., and Gresillon, J. M.: Modeling all exceedances above a
643 threshold using an extremal dependence structure: Inferences on several flood characteristics,
644 Water Resources Research, 45, W03407, 10.1029/2007wr006322, 2009.
645 Rieder, H. E., Staehelin, J., Maeder, J. A., Peter, T., Ribatet, M., Davison, A. C., Stübi, R.,
646 Weihs, P., and Holawe, F.: Extreme events in total ozone over Arosa - Part 2: Fingerprints of
647 atmospheric dynamics and chemistry and effects on mean values and long-term changes,
648 Atmospheric Chemistry and Physics 10, 10033-10045, 2010a.
649 Rieder, H. E., Staehelin, J., Maeder, J. A., Peter, T., Ribatet, M., Davison, A. C., Stübi, R.,
650 Weihs, P., and Holawe, F.: Extreme events in total ozone over Arosa - Part 1: Application of
651 extreme value theory, Atmospheric Chemistry and Physics 10, 10021-10031, 2010b.
652 Rieder, H. E., Jancso, L. M., Di Rocco, S., Staehelin, J., Maeder, J. A., Peter, T., Ribatet, M.,
653 Davison, A. C., De Backer, H., Koehler, U., Krzyscin, J., and Vanicek, K.: Extreme events in
654 total ozone over the Northern mid-latitudes: an analysis based on long-term data sets from
655 five European ground-based stations, Tellus Series B-Chemical and Physical Meteorology,
656 63, 860-874, 10.1111/j.1600-0889.2011.00575.x, 2011.
657 Rieder, H. E., Frossard, L., Ribatet, M., Staehelin, J., Maeder, J. A., Di Rocco, S., Davison, A.
658 C., Peter, T., Weihs, P., and Holawe, F.: On the relationship between total ozone and
659 atmospheric dynamics and chemistry at mid-latitudes - Part 2: The effects of the El
660 Nino/Southern Oscillation, volcanic eruptions and contributions of atmospheric dynamics and
661 chemistry to long-term total ozone changes, Atmospheric Chemistry and Physics, 13, 165-
662 179, 10.5194/acp-13-165-2013, 2013.
663 Rigby, M., Prinn, R. G., O'Doherty, S., Montzka, S. A., McCulloch, A., Harth, C. M., Muhle,
664 J., Salameh, P. K., Weiss, R. F., Young, D., Simmonds, P. G., Hall, B. D., Dutton, G. S.,
665 Nance, D., Mondeel, D. J., Elkins, J. W., Krummel, P. B., Steele, L. P., and Fraser, P. J.: Re-
666 evaluation of the lifetimes of the major CFCs and CH3CCl3 using atmospheric trends,
667 Atmospheric Chemistry and Physics, 13, 2691-2702, DOI 10.5194/acp-13-2691-2013, 2013.

668 Robock, A.: Volcanic eruptions and climate, Reviews of Geophysics, 38, 191-219, 2000.
669 Schnadt Poberaj, C., Staehelin, J., and Brunner, D.: Missing stratospheric ozone decrease at
670 southern hemisphere middle latitudes after Mt. Pinatubo: A dynamical perspective, J. Atmos.
671 Sci., 68, 1922-1945, 2011.
672 Schwartz, M. J., Manney, G. L., Hegglin, M. I., Liversey, N. J., Santee, M. L., and Daffer, W.
673 H.: Climatology and variability of trace gases in extratropical double-tropopause regions from
674 MLS, HIRDLS and ACE-FTS measurements, Journal of Geophysical Research -
675 Atmospheres, submitted.
676 Seidel, D. J., Fu, Q., Randel, W. J., and Reichler, T. J.: Widening of the tropical belt in a
677 changing climate, Nature Geoscience, 1, 21-24, 10.1038/ngeo.2007.38, 2008.
678 Shepherd, T. G.: Dynamics, stratospheric ozone, and climate change, Atmosphere-Ocean, 46,
679 117-138, 10.3137/ao.460106, 2008.
680 Solomon, S.: Stratospheric ozone depletion: A review of concepts and history, Reviews of
681 Geophysics, 37, 275-316, 1999.
682 SPARC-CCMVal: SPARC Report on the Evaluation of Chemistry-Climate Models, 2010.
683 Steinbrecht, W., Claude, H., Kohler, U., and Hoinka, K. P.: Correlations between tropopause
684 height and total ozone: Implications for long-term changes, Journal of Geophysical Research-
685 Atmospheres, 103, 19183-19192, 1998.
686 Thompson, D. W. J., and Wallace, J. M.: Annular modes in the extratropical circulation. Part
687 I: Month-to-month variability, Journal of Climate, 13, 1000-1016, 2000.
688 Tourpali, K., Bais, A. F., Kazantzidis, A., Zerefos, C. S., Akiyoshi, H., Austin, J., Bruhl, C.,
689 Butchart, N., Chipperfield, M. P., Dameris, M., Deushi, M., Eyring, V., Giorgetta, M. A.,
690 Kinnison, D. E., Mancini, E., Marsh, D. R., Nagashima, T., Pitari, G., Plummer, D. A.,
691 Rozanov, E., Shibata, K., and Tian, W.: Clear sky UV simulations for the 21st century based
692 on ozone and temperature projections from Chemistry-Climate Models, Atmospheric
693 Chemistry and Physics, 9, 1165-1172, 2009.

694 Trenberth, K. E.: Progress during TOGA in understanding and modeling global
695 teleconnections associated with tropical sea surface temperatures, J. Geophys. Res., 103,
696 14291-14324, 1998.
697 WMO: Scientific Assessment of Ozone Depletion: 2006, Global Ozone Research and
698 Montitoring Project 50, 572, 2007.
699 WMO: Scientific Assessment of Ozone Depletion: 2010, Global Ozone Research and
700 Montitoring Project 50, 516, 2011.
701 Wohltmann, I., Lehmann, R., Rex, M., Brunner, D., and Mader, J. A.: A process-oriented
702 regression model for column ozone, Journal of Geophysical Research-Atmospheres, 112,
703 D12304, 10.1029/2006jd007573, 2007.
704 Ziemke, J. R., Chandra, S., Oman, L. D., and Bhartia, P. K.: A new ENSO index derived from
705 satellite measurements of column ozone, Atmospheric Chemistry and Physics, 10, 3711-3721,
706 2010.
707
708
709
710
711
712
713
714
715
716

Table 1: Correlation of the NAO-Index and the average number (#) of EHOs and ELOs and mean column ozone (TOC) on seasonal basis at the five US long-term total ozone monitoring sites.

	Correlation with NAO Index		
season/station	**# EHOs**	**# ELOs**	**Mean TOC**
DJF			
BISMARCK	-0.44	0.40	-0.53
BOULDER	-0.26	0.29	-0.34
CARIBOU	-0.53	0.33	-0.61
WALLOPS ISLAND	-0.28	0.38	-0.52
NASHVILLE	-0.53	0.33	-0.48
MAM			
BISMARCK	-0.21	0.22	-0.29
BOULDER	-0.10	0.10	-0.21
CARIBOU	-0.16	0.10	-0.21
WALLOPS ISLAND	-0.10	0.23	-0.21
NASHVILLE	-0.27	0.10	-0.20

Table 2: Seasonal linear trends (in % per decade) for observed and extremes removed winter (DJF) and spring (MAM) column ozone time series in 1970-1995 and 1996-2010 at the five US ozone monitoring sites. Standard errors are given in parentheses, p-values are provides as superscript.

	trend (in % per decade)			
	1970-1995		1996-2010	
season/station	observations	no extremes	observations	no extremes
DJF				
Bismarck	-2.9 (±0.8) $^{0.001}$	-1.3 (±0.4) $^{0.005}$	+3.6 (±2.2) $^{0.127}$	+2.0 (±1.3) $^{0.145}$
Boulder	-2.8 (±0.8) $^{0.002}$	-1.3 (±0.5) $^{0.034}$	+1.3 (±1.9) $^{0.532}$	+0.2 (±1.0) $^{0.897}$
Caribou	-3.8 (±1.1) $^{0.003}$	-0.9 (±0.7) $^{0.205}$	+3.1 (±2.4) $^{0.277}$	+2.1 (±2.0) $^{0.308}$
Wallops Island	-2.9 (±1.1) $^{0.017}$	-0.7 (±0.6) $^{0.434}$	+3.8 (±2.4) $^{0.136}$	+2.0 (±1.1) $^{0.142}$
Nashville	-2.6 (±1.0) $^{0.016}$	-1.3 (±0.6) $^{0.023}$	+2.5 (±2.2) $^{0.294}$	+0.5 (±1.1) $^{0.658}$
MAM				
Bismarck	-4.8 (±0.7) $^{0.001}$	-2.3 (±0.5) $^{0.001}$	+0.8 (±1.8) $^{0.685}$	+0.3 (±1.1) $^{0.890}$
Boulder	-4.3 (±0.9) $^{0.001}$	-2.3 (±0.5) $^{0.001}$	+1.2 (±1.9) $^{0.535}$	+0.6 (±0.9) $^{0.532}$
Caribou	-3.2 (±1.1) $^{0.004}$	-1.7 (±0.5) $^{0.004}$	-1.1 (±1.2) $^{0.395}$	-0.5 (±0.8) $^{0.225}$
Wallops Island	-3.5 (±1.0) $^{0.001}$	-1.9 (±0.6) $^{0.003}$	-0.2 (±2.2) $^{0.928}$	+0.0 (±1.2) $^{0.993}$
Nashville	-3.2 (±1.0) $^{0.005}$	-1.9 (±0.6) $^{0.003}$	+3.6 (±2.1) $^{0.101}$	+1.0 (±1.1) $^{0.258}$

738 Table 3: Pattern correlation of the net influence of extremes on winter (DJF) and spring
739 (MAM) mean column ozone among the five US ozone monitoring sites. * For station code see
740 Figure 1.

Season/Stations					
DJF	BIS	BDR	CAR	WAI	BNA
BIS	X	0.64	0.48	0.42	0.6
BDR	0.64	X	0.51	0.34	0.58
CAR	0.48	0.51	X	0.69	0.63
WAI	0.42	0.34	0.69	X	0.69
BNA	0.6	0.58	0.63	0.69	X
MAM					
BIS	X	0.76	0.69	0.59	0.6
BDR	0.76	X	0.61	0.68	0.65
CAR	0.69	0.61	X	0.5	0.52
WAI	0.59	0.68	0.5	X	0.72
BNA	0.6	0.65	0.52	0.72	X

741

742

743

744

745

746

747

748

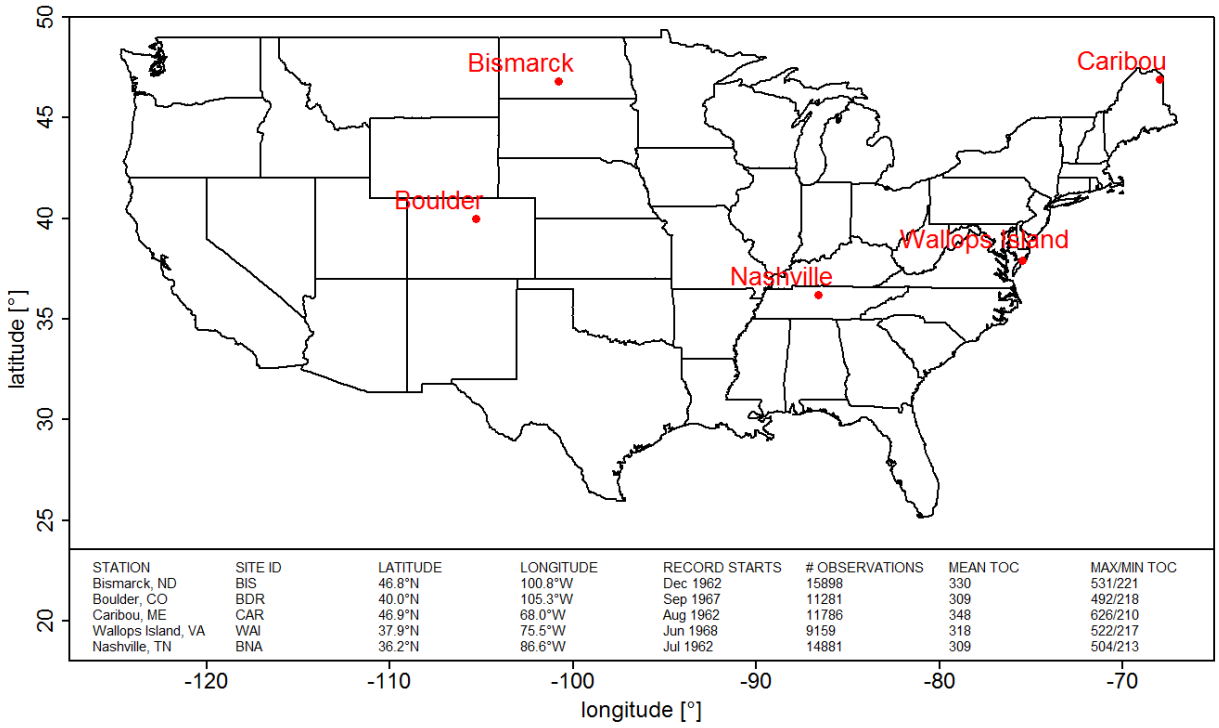

STATION	SITE ID	LATITUDE	LONGITUDE	RECORD STARTS	# OBSERVATIONS	MEAN TOC	MAX/MIN TOC
Bismarck, ND	BIS	46.8°N	100.8°W	Dec 1962	15898	330	531/221
Boulder, CO	BDR	40.0°N	105.3°W	Sep 1967	11281	309	492/218
Caribou, ME	CAR	46.9°N	68.0°W	Aug 1962	11786	348	626/210
Wallops Island, VA	WAI	37.9°N	75.5°W	Jun 1968	9159	318	522/217
Nashville, TN	BNA	36.2°N	86.6°W	Jul 1962	14881	309	504/213

Figure 1: Geographical overview and site specific information for the US long-term Dobson total ozone monitoring sites.

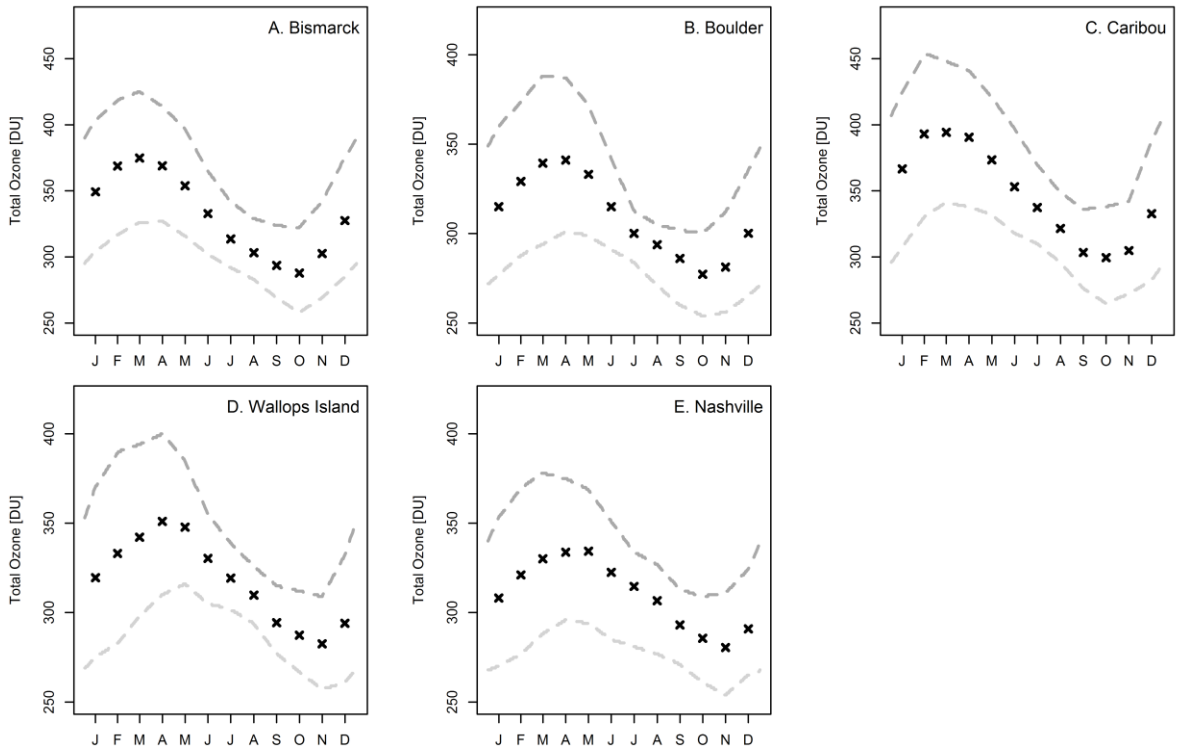

762

763 Figure 2: Thresholds for extreme highs (EHOs, dark grey dashed lines) and lows (ELOs, light
764 grey dashed lines) of total ozone and climatological monthly means of total ozone (black
765 crosses) at (A) Bismarck, (B) Boulder, (C) Caribou, (D) Wallops Island and (E) Nashville.

766

767

768

769

770

771

772

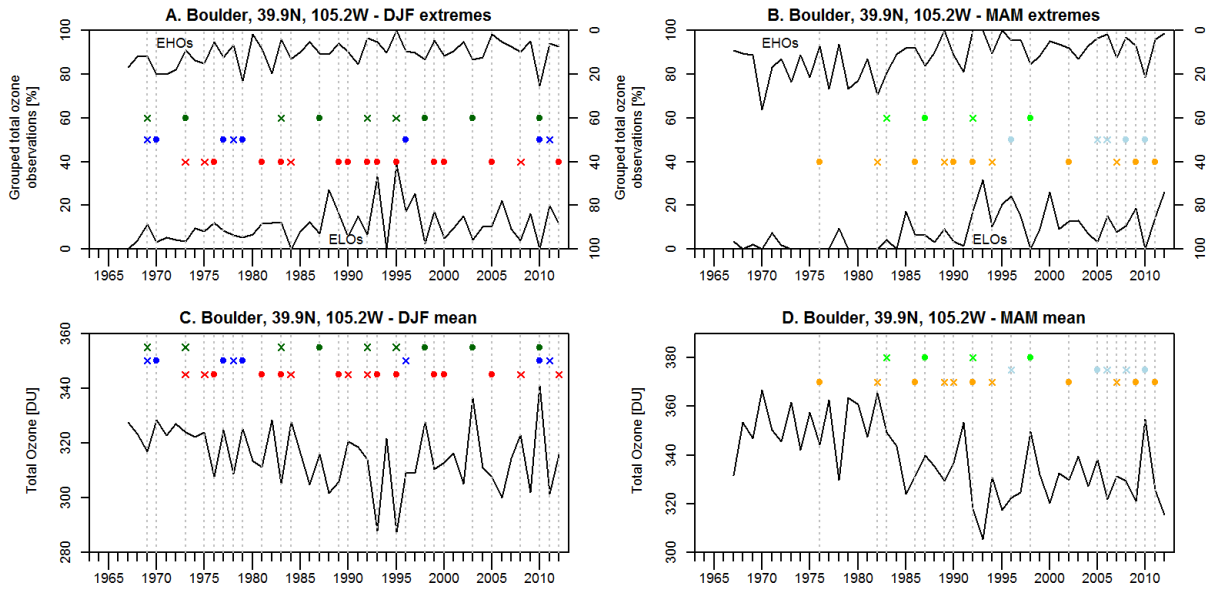

Figure 3: 'Fingerprints' of the NAO and ENSO as detected for Boulder in the seasonal frequency time series of EHOs (right axis, top to bottom) and ELOs (left axis, bottom to top) for (A) winter (DJF), and (B) spring (MAM). Bottom panels (C) and (D) show 'fingerprints' in seasonal mean column ozone. Filled circles denote visible 'fingerprints' and crosses denote not visible 'fingerprints'. NAO positive (negative) phase is indicated for winter in red (blue) and for spring in orange (light blue), ENSO positive phase is indicated for winter (spring) in green (light green).

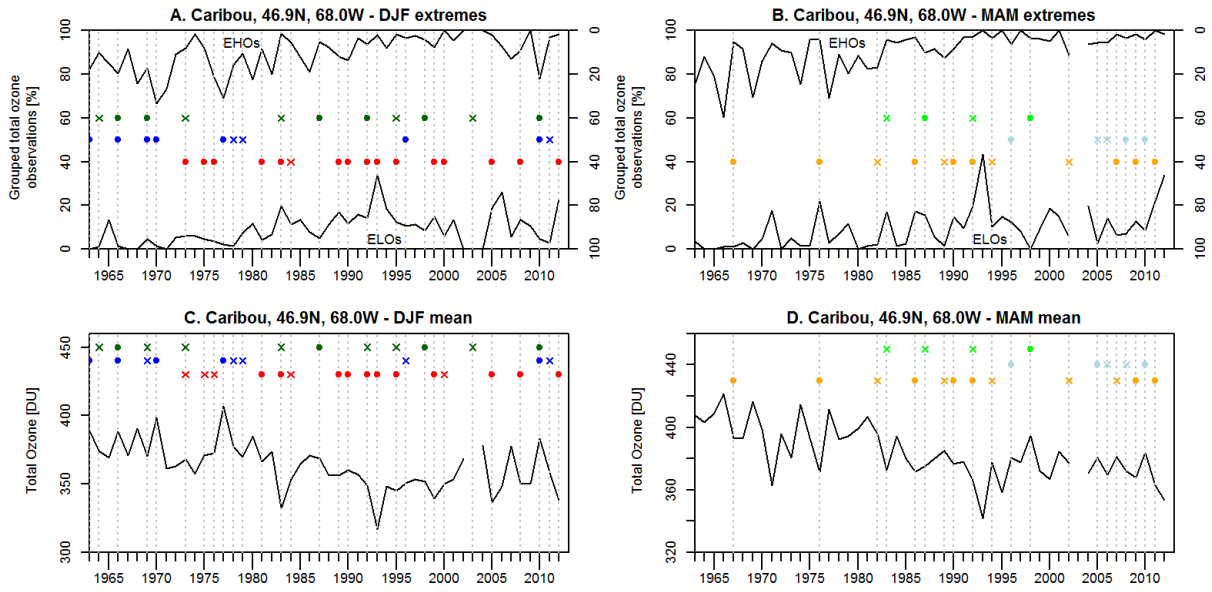

Figure 4: as Figure 3 but for Caribou.

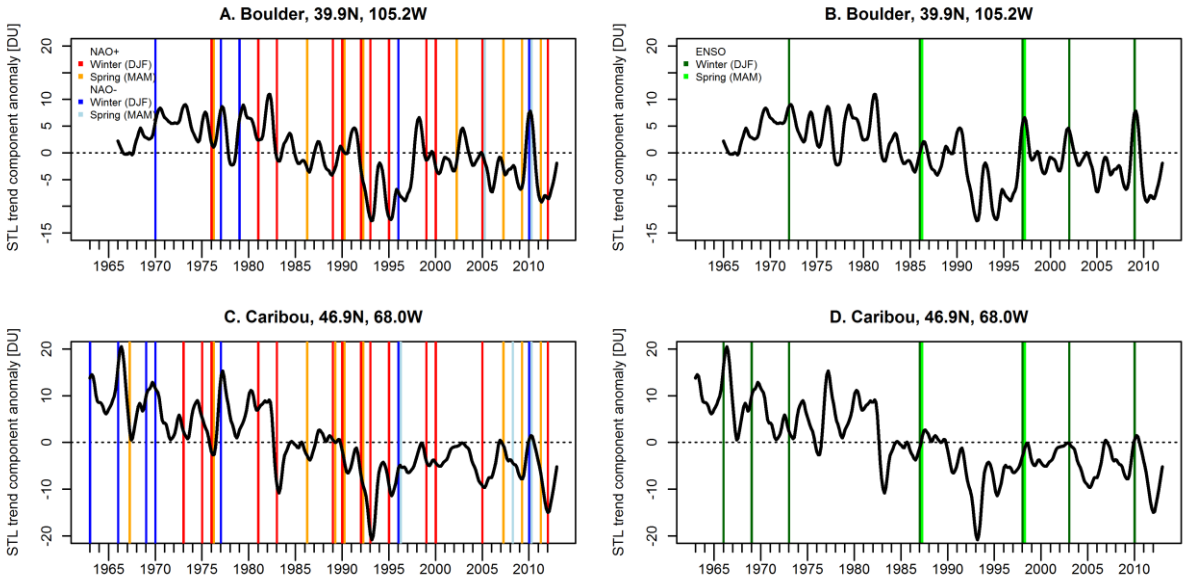

Figure 5: STL-trend component anomaly (in DU) in 1963-2012 for Boulder (top) and Caribou (bottom) with underlying marks (colored vertical bars) for 'fingerprints' of positive and negative NAO modes (left panels) and warm ENSO phases (right panels) on seasonal basis. NAO positive (negative) phase is indicated for winter in red (blue) and for spring in orange (light blue). Warm ENSO phase is indicated for winter in green and spring in light green.

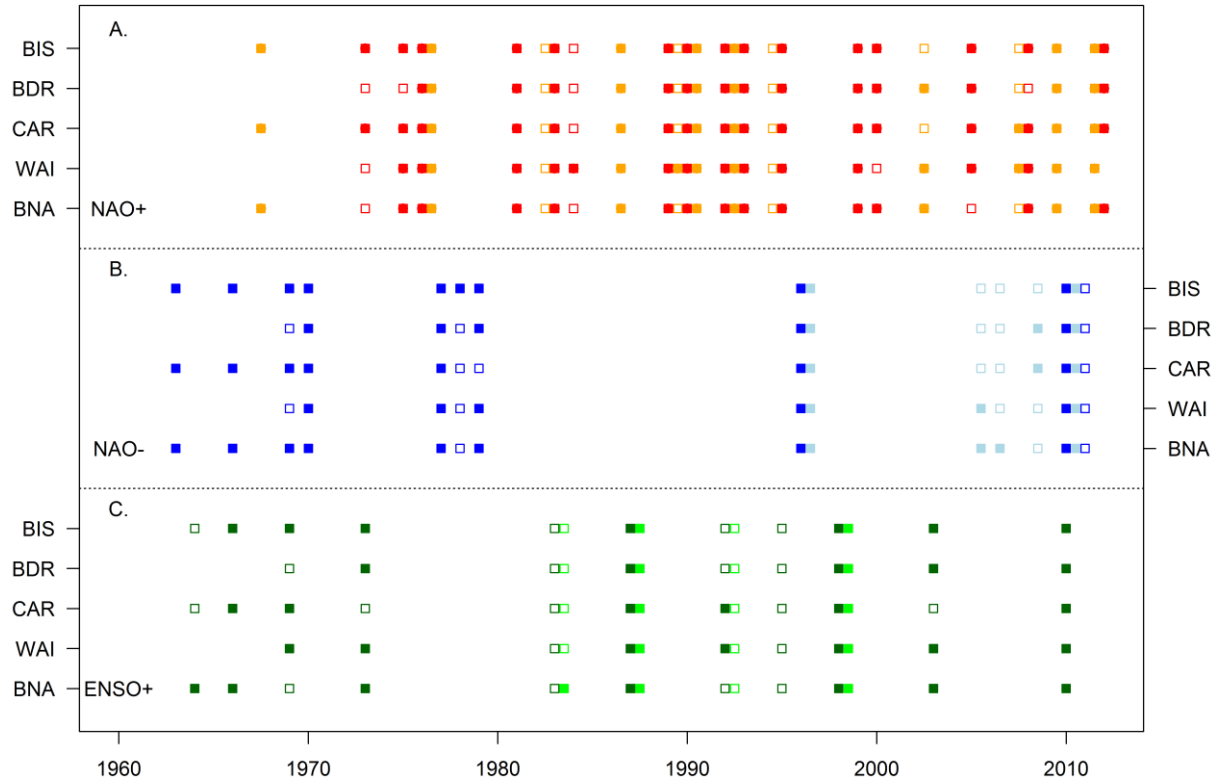

Figure 6: Summary of detected and missed 'fingerprints' at all five US stations for (A) the NAO in its positive phase (winter red, spring orange), (B) the NAO in its negative phase (winter blue, spring light blue), and (C) ENSO in its warm phase (winter green, spring light green). Filled squares mark visible 'fingerprints' while open squares mark not visible 'fingerprints'.

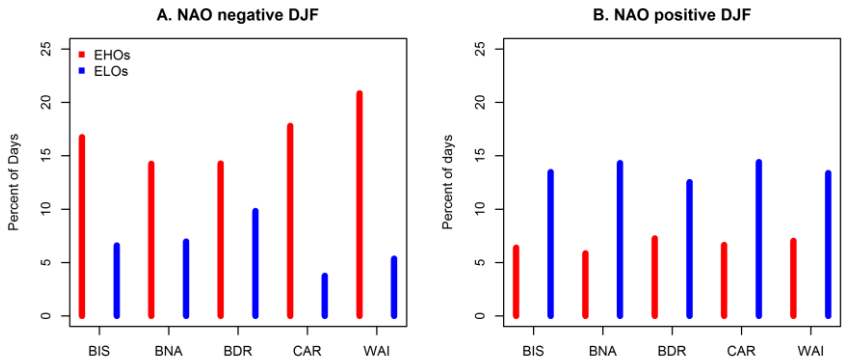

Figure 7: Average fraction of days (in %) identified as EHO and ELO during (a) negative and (b) positive NAO phase in winter (DJF) season.

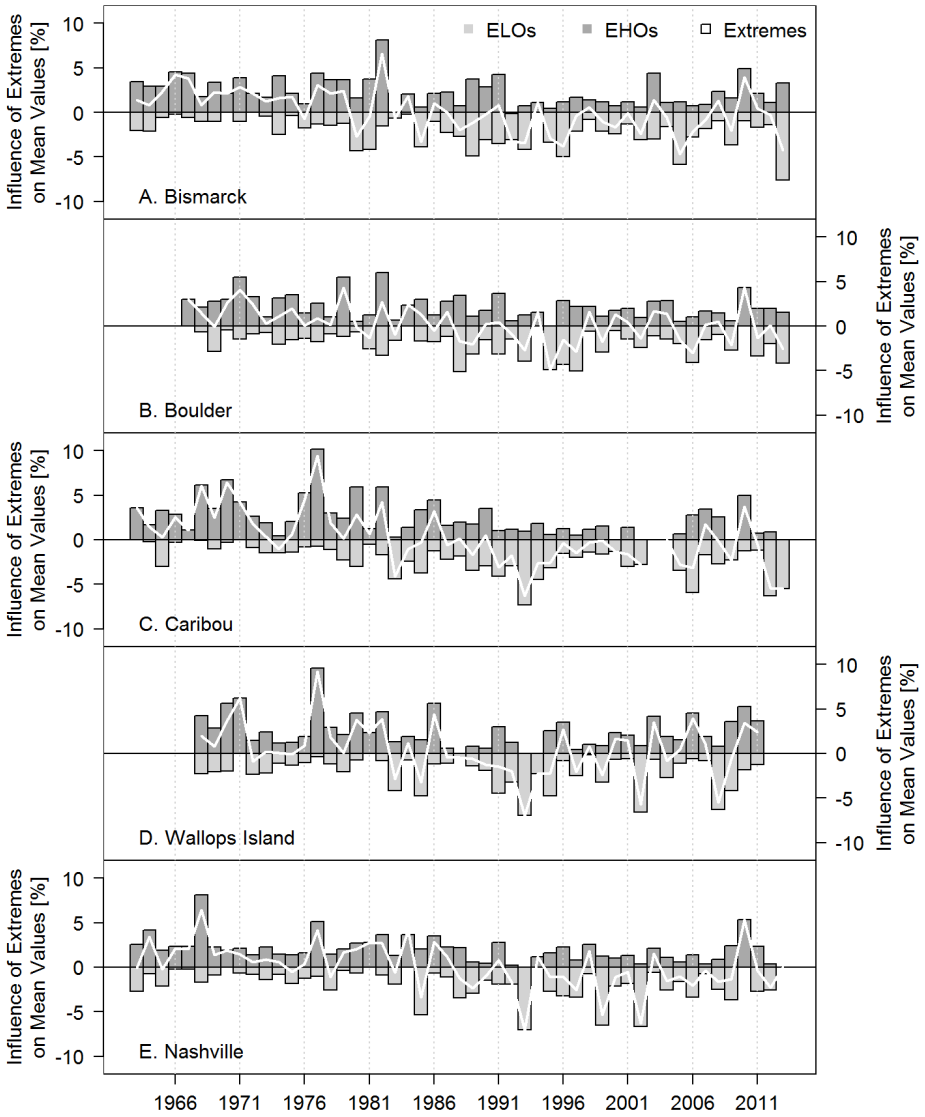

Figure 8: Influence (in %) of extreme low (ELOs, light histogram) and high (EHOs, dark histogram) ozone events and net influence of extremes (white curve) on winter (DJF) mean ozone at (A) Bismarck, (B) Boulder, (C) Caribou, (D) Wallops Island, and (E) Nashville.

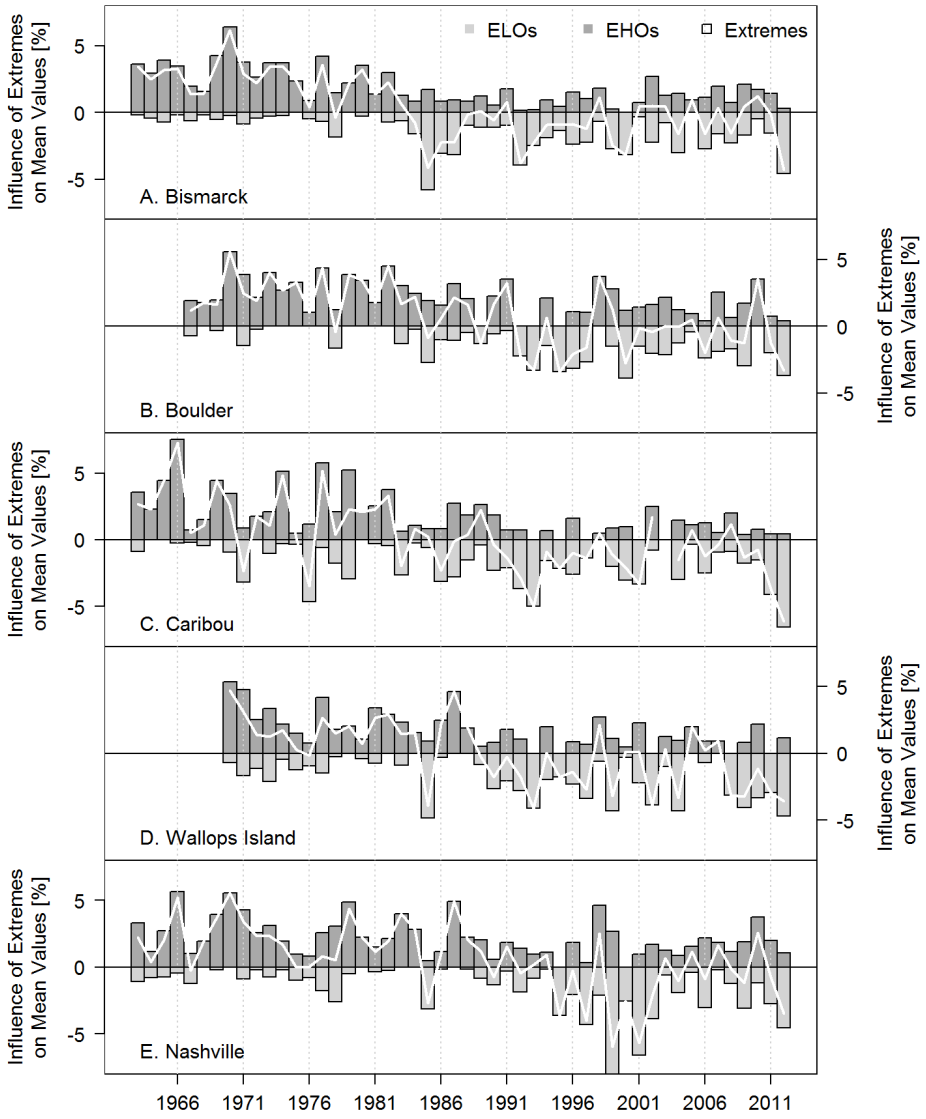

Figure 9: as Figure 8 but for spring (MAM).